

# Epidemic Spreading and Aging in Temporal Networks with Memory

Michele Tizzani and Raffaella Burioni

*Dipartimento di Scienze Matematiche, Fisiche e Informatiche,  
Università degli Studi di Parma, Parco Area delle Scienze, 7/A 43124 Parma, Italy and  
INFN, Gruppo Collegato di Parma, Parco Area delle Scienze 7/A, 43124 Parma, Italy*

Simone Lenti

*Dipartimento di Fisica, "Sapienza" Università di Roma, P.le A. Moro 2, I-00185 Roma, Italy*

Enrico Ubaldi

*ISI Foundation, 10126 Torino, Italy*

Alessandro Vezzani

*Istituto dei Materiali per l'Elettronica ed il Magnetismo (IMEM-CNR),  
Parco Area delle Scienze, 37/A-43124 Parma, Italy and  
Dipartimento di Scienze Matematiche, Fisiche e Informatiche,  
Università degli Studi di Parma, Parco Area delle Scienze, 7/A 43124 Parma, Italy*

Claudio Castellano

*Istituto dei Sistemi Complessi (ISC-CNR), via dei Taurini 19, I-00185 Roma, Italy and  
Dipartimento di Fisica, "Sapienza" Università di Roma, P.le A. Moro 2, I-00185 Roma, Italy*

(Dated: December 20, 2018)

Time-varying network topologies can deeply influence dynamical processes mediated by them. Memory effects in the pattern of interactions among individuals are also known to affect how diffusive and spreading phenomena take place. In this paper we analyze the combined effect of these two ingredients on epidemic dynamics on networks. We study the susceptible-infected-susceptible (SIS) and the susceptible-infected-removed (SIR) models on the recently introduced activity-driven networks with memory. By means of an activity-based mean-field approach we derive, in the long time limit, analytical predictions for the epidemic threshold as a function of the parameters describing the distribution of activities and the strength of the memory effects. Our results show that memory reduces the threshold, which is the same for SIS and SIR dynamics, therefore favouring epidemic spreading. The theoretical approach perfectly agrees with numerical simulations in the long time asymptotic regime. Strong aging effects are present in the preasymptotic regime and the epidemic threshold is deeply affected by the starting time of the epidemics. We discuss in detail the origin of the model-dependent preasymptotic corrections, whose understanding could potentially allow for epidemic control on correlated temporal networks.

## I. INTRODUCTION

In many social and information systems, the time scales for the evolution of the interaction network are often comparable to the time scales of the dynamical processes taking place on top of them [1]. The diffusion of online information or the spreading of transmitted diseases in a population are typical examples of such processes, for which a focus on a static representation of the network is not able to capture the very influence of the rapidly varying topology [2–7]. Besides, recent advances in technology have allowed to measure and monitor the evolution of interactions with an unprecedented time resolution [8], calling for new theories to understand the effect of time-varying topologies on dynamical processes.

Interactions and the creation of links are generated by the agents activity, a quantity that can be easily measured from available large scale and time resolved datasets [9]. An interesting line of modelling has developed, aiming at including explicitly the effect of activity distributions on network dynamics: activity-driven net-

works [10]. In activity-driven models, each agent is endowed with a degree of freedom that encodes the propensity of the individual to engage in a social event, establishing a link with another agent in the system. Notably, measured activities are typically highly heterogeneous and this has strong effects on network evolution.

When links are randomly established among agents, activity-driven models have been studied in detail [10–13], uncovering the effects of heterogeneous activity distributions on network topology and on dynamical processes, such as random walks and epidemic processes.

However, in general agents do not connect randomly to their peers [14–16]. During their activity, individuals remember their friends and their social circles and they are more inclined to interact with already known pals, establishing strong and weak ties with their peers [17, 18]. Recent works have tackled this problem by applying a data-driven approach. A tie allocation mechanism in real systems has been measured, introducing a memory process on top of activity-driven models [19, 20]. As reasonably expected, social interactions are not randomly estab-

lished but they are rather concentrated towards already contacted nodes, with a reinforcement process encoded in a single measurable memory parameter. The memory process tunes the network evolution, that can be predicted at large times [21–23], and it is also expected to influence dynamical processes. Non-Markovian dynamics can indeed change the spreading rate in a diffusion process, slowing it down in some cases and speeding it up in others [24–30]. Disparate effects have been shown to occur also in epidemic spreading on activity-driven networks, where memory can lower or increase the epidemic threshold in SIS or SIR model, respectively [31]. This happens when the epidemic process and the network evolution start at the same time. However, the network evolution in the presence of non-Markovian effects could introduce aging in the process [32], as usually observed in processes with memory also in other fields [33], and this could further influence the spreading dynamics.

In this paper, we analyze in detail SIS and SIR epidemic processes on activity-driven time-varying networks in the presence of memory. Introducing an *activity-based mean-field* (ABMF) approximation, we derive analytically, as a function of the activity distribution and of the parameter tuning the memory, a prediction for the threshold, holding both for the SIS and the SIR models. The result shows that memory overall reinforces the effects of activity fluctuations, leading to a lower value for the epidemics threshold. We prove that ABMF approximation is equivalent to an epidemic model defined on an effective static network, that we also investigate. Numerical simulations evidence that ABMF approach provides exact results when the epidemics start after the network has evolved for a long time. In this regime indeed mean field holds since agents have been connected to a large number of pairs, while the creation of new links becomes negligible.

We show however that strong aging effects are present in the preasymptotic regime and the epidemic threshold is deeply affected by the starting time of the epidemics. In particular, at weak memory the creation of new links cannot be discarded and this increases the epidemic threshold according to the memoryless predictions. On the other hand, for strong memory, at short times the dynamics displays correlations among infection probabilities of nodes which have already been in contact. The correlations give rise to backtracking effects that cannot be ignored. In this case, typically the threshold of the SIS and SIR models are respectively smaller and larger with respect to the mean-field prediction. We explain in detail the origin of such deviations, opening new perspectives for epidemic control of disease and information spreading on temporal networks with high correlations.

The paper is organized as follows. In Section II we first summarize the activity-driven model for network topology in the presence of memory and then define epidemic dynamics on top of it. In the next Section, after a brief recapitulation of the analytical approach to epidemic dynamics on memoryless activity-driven networks,

we describe in detail how the approach is modified to deal with networks with memory, deriving predictions for the epidemic threshold. In Section IV we compare analytical predictions with numerical results, obtained by considering both an effective static network and the full time-evolution of the topology. The final Section presents some concluding remarks and perspectives for future work.

## II. THE MODEL

### A. Activity-Driven Networks with memory

In activity-driven models [10], each node  $v_i$  ( $i = 1, \dots, N$ ) of the graph  $G_t$  has an activity  $a_i$  assigned randomly according to a given distribution  $F(a)$ . The dynamics occurs over discrete temporal steps of length  $\Delta t$ . At each step, with probability  $a_i \Delta t$  the vertex  $v_i$  becomes active and gets linked to  $m$  other vertices. Connections last for a temporal interval  $\Delta t$ . At the next time step  $t + \Delta t$  all existing edges are deleted and the procedure is iterated. Note that the activity  $a$  has the dimensions of a probability per unit time. Real data observations indicate that human interactions are very often characterized by skewed and long tailed activity distributions [10] so  $F(a)$  is typically assumed to be a power-law,  $F(a) = Ba^{-(\nu+1)}$  with  $\varepsilon \leq a_i \leq A$ . Since in our simulations we will keep the time interval  $\Delta t = 1$ , the upper cutoff is naturally set to  $A = 1$ .

In order to take into account the tendency of individuals to persist in their social connections, a “reinforcement” mechanism has recently been introduced in activity-driven models [19, 21]. The nodes are endowed with a memory of their previous contacts and they have a propensity to establish contacts preferably with individuals belonging to their social circle. For an active node  $v_i$ , which has already contacted  $k_i(t)$  different nodes at time  $t$ , this process is described by assuming that the node connects with a new node with probability

$$p[k_i(t)] = [1 + k_i(t)/c_i]^{-\beta_i}, \quad (1)$$

while it establishes a connection with a previously contacted node with complementary probability  $1 - p[k_i(t)]$ . The probability depends on the degree of the integrated network at time  $t$ ,  $k_i(t)$ , i.e, the number of nodes that  $v_i$  has contacted up to time  $t$ . We will call  $A_{ij}(t)$  the adjacency matrix of this integrated network. The parameter  $\beta_i > 0$  tunes the memory process. For  $\beta_i \approx 0$  the probability  $p[k_i(t)] \approx 1$  weakly depends on the growing degree  $k_i(t)$ , while, at large  $\beta_i$ ,  $p[k_i(t)]$  rapidly decays with of  $k_i(t)$ . The constant  $c_i$  sets an intrinsic value for the number of connections that node  $v_i$  is able to engage in before memory effects become relevant. Empirical measures on several datasets [21] are compatible with constant values of  $\beta_i = \beta$  and  $c_i = c$ , so that the function  $p(\cdot)$  turns out to be independent of  $i$ . In particular, the exponent  $\beta$  ranges from  $\beta \approx 0.15$  in the citation networks, to  $\beta \approx 0.5$

in Twitter mentions and to  $\beta \approx 1.2$  in the mobile phone calls. In this paper we study the dependence of the epidemic threshold on the value of the exponent  $\beta$ , while we set  $c = 1$  and  $m = 1$ , with no loss of generality.

As shown in Ref. [21] the asymptotic form of the degree distribution for the integrated network can be derived analytically. In particular, in the regime  $1 \ll k \ll N$  the degree of nodes of activity  $a$  is narrowly distributed around the average value

$$\bar{k}(a, t) = C(a)t^{1/(1+\beta)}, \quad (2)$$

i.e. the degree of each node increases sublinearly in time, with a prefactor depending on its activity. The prefactor  $C(a)$  is determined by the condition

$$\frac{C(a)}{1+\beta} = \frac{a}{C^\beta(a)} + \int da \frac{F(a)a}{C^\beta(a)}. \quad (3)$$

In the memoryless case  $\beta = 0$ , where an active node connects always with a randomly chosen vertex, Eq. (3) gives  $C(a) = a + \langle a \rangle$  recovering the result of [34]. Hereafter we will denote in general with  $\langle g \rangle = \int da F(a)g(a)$  the average of a function of the activity  $g(a)$  over the network.

### B. The epidemic process

We now turn to the spreading of infectious diseases on activity-driven temporal networks with memory. We start by considering the standard Susceptible-Infected-Susceptible (SIS) model, the simplest description of a disease not conferring immunity. In the SIS model nodes can be in two states, either susceptible (S) or infectious (I). An infected node can turn spontaneously susceptible with rate  $\mu$ , while an infected node transmits the infection over an edge to a susceptible neighbor with rate  $\lambda$ . The two elementary events are therefore:



In the Susceptible-Infected-Recovered (SIR) model the disease confers immunity, so that the nodes can be in three states susceptible (S), infectious (I) and recovered (R) which are immune to a new infection. The dynamics is described by the following reaction scheme:



The epidemic process on activity-driven networks is implemented by iterating discrete time steps of duration  $\Delta t$ :

- at the beginning of each time step there are  $N$  disconnected vertices;
- with probability  $a_i \Delta t$  a vertex  $v_i$  becomes active and connects to a previously linked node with probability  $1 - p(k_i)$ , or with a new node  $v_j$  with probability  $p(k_i)$ , in this second case  $k_i(t)$ ,  $k_j(t)$  and  $A_{ij}(t)$  are increased by one unit;

- if one of the nodes connected by the link is infected and the other one is susceptible, the susceptible becomes infected with probability  $\lambda$ ;
- a vertex  $v_j$ , if infected, becomes susceptible (SIS), or recovers (SIR) with probability  $\mu \Delta t$ .

In activity-driven models,  $\lambda$  is a pure number, i.e. the probability that in a single contact the infection is actually transmitted, while  $\mu$  is still the rate of recovery for a single individual. Ignoring the inhomogeneity in the activities, one can estimate the total rate for the infection process per node as  $\lambda \langle k' \rangle$ , where  $\langle k' \rangle = 2 \langle a \rangle$  is the average degree per unit time; this is the quantity to be compared with the recovery rate per node  $\mu$ .

## III. ANALYTICAL RESULTS

### Epidemics on memoryless activity-driven networks

The epidemic spreading for the memoryless case  $\beta = 0$  has been studied in [10] adopting an ABMF approach. The epidemic state of a node, when averaged over all possible dynamical evolutions, only depends on the value of its activity  $a_i$ . In particular, one can define the probability  $\rho(a_i, t)$  that a node with activity  $a_i$  is infected at time  $t$ . The corresponding evolution equation is:

$$\partial_t \rho(a_i) = -\mu \rho(a_i) + \lambda [1 - \rho(a_i)] \frac{1}{N-1} \sum_{j \neq i} [a_i \rho(a_j) + a_j \rho(a_j)]. \quad (6)$$

The first term on the right side is due to recovery events; the second term takes into account the event that a susceptible node of class  $a_i$  becomes active and contracts the disease by connecting to an infected individual, while the third term is the analogous term for the case of a susceptible node that, independently of her own activity, is contacted by an infected active individual.

The description in terms of quantities that only depend on the activity is conceptually analogous to the heterogeneous-mean-field approach for dynamical processes on static networks [35]. In that case, one assumes that the only property determining the epidemic state of a node is the degree  $k$  and then derives equations for the probabilities  $\rho_k$ . An important difference must however be stressed. Assuming the epidemic state to depend only on the degree is an approximation for static networks, because it neglects the quenched nature of the network structure that makes properties of nodes, with the same degree but embedded in different local environments, different. In practice, this assumption is equivalent to replacing the actual adjacency matrix of the network ( $A_{ij}$  equal to 0 or 1 depending on the presence of the connection between  $v_i$  and  $v_j$ ) with an annealed adjacency matrix  $P_{ij} = k_i k_j / (\langle k \rangle N)$  [36], expressing the probability that vertices  $v_i$  and  $v_j$  with degree  $k_i$  and  $k_j$  are connected. The annealed approach is an approximation

for static networks, while it is exact for networks where connections are continuously reshuffled at each time step of the dynamics, since the reshuffling process destroys local correlations. Since in memoryless activity-driven networks connections are extracted anew at each time step, the ABMF approach provides exact results in this case.

Equation (6) can be analyzed by means of a linear stability analysis, yielding, for large  $N$ , the threshold [10]

$$\left(\frac{\lambda}{\mu}\right)_{\text{ML}} = \frac{1}{\langle a \rangle + \sqrt{\langle a^2 \rangle}}. \quad (7)$$

The same result can be derived for the SIR case.

## Epidemics on activity-driven networks with memory

### Individual-based mean-field approach

In presence of memory, interactions occur preferably with a subset of the other nodes (the social circle) creating correlations. Therefore, we implement a different, individual-based, mean-field approach, keeping explicitly track of the evolution of social contacts (i.e. of the memory). Let us first consider the SIS model. The observable of interest is the probability  $\rho_i(t)$  that node  $v_i$  is infected at time  $t$ . Its evolution can be written as

$$\partial_t \rho_i(t) = -\mu \rho_i(t) + \lambda [1 - \rho_i(t)] \left\{ \sum_j a_i [1 - p(k_i)] \frac{A_{ij}(t)}{k_i} \rho_j(t) + \sum_{j \approx i} a_i p(k_i) \frac{1}{N - k_i - 1} \rho_j(t) + \sum_j a_j [1 - p(k_j)] \frac{A_{ij}(t)}{k_j} \rho_j(t) + \sum_{j \approx i} a_j p(k_j) \frac{1}{N - k_j - 1} \rho_j(t) \right\} \quad (8)$$

Here  $j \approx i$  indicates the sum over the nodes  $j$  not yet connected to  $i$ ,  $N - k_j(t) - 1$  is their number. The quantity  $A_{ij}(t)$  is the adjacency matrix of the time-integrated network at time  $t$ , i.e., it is equal to 1 if  $v_i$  and  $v_j$  have been in contact at least once in the past and 0 otherwise. In Eq. (8), the only approximation made is that the dynamical state of every node is considered to be independent of the state of the partner in the interaction; in other words, we neglect the existence of dynamical correlations among nodes, which are created by the partially quenched nature of the interaction pattern due to memory. It is exactly the same approximation that is involved by the individual-based mean-field approach for static networks [37].

The first term on the right hand side of Eq. (8) is the recovery rate of  $\rho_i(t)$ . The second term, describing the infection process, is the product of  $\lambda$  times the probability for  $v_i$  to be susceptible and, in curly brackets, the fraction of infected nodes contacted by  $v_i$  per unit time. In the curly brackets, the first and the second term describe the case where  $v_i$  is active and connects to the infected node  $v_j$  taking into account that the link can be an old or a new one respectively. In the same way, the third and the fourth term represent the probabilities that  $v_i$  is contacted by an infected and active node  $v_j$ .

Since both  $A_{ij}(t)$  and  $k_i(t)$  depend on the evolution time  $t$ , the behavior of the epidemics can strongly depend on the starting time of the outbreak, giving rise to aging effects that will be investigated in numerical simulations. When the epidemic starts at very large times, an analytic approach can be considered. In this regime, with  $1 \ll k_i(t) \ll N$ , we expect that the creation of new

contacts can be ignored and that the dynamical correlations are asymptotically negligible, since the connectivity of the integrated network becomes large. If the epidemic starts at very large times, therefore, we can apply an heterogeneous mean-field approximation for  $A_{ij}(t)$ , allowing for an analytical solution of the problem which we expect to be asymptotically exact.

### The behavior for large times

Let us consider the regime of large times, where  $1 \ll k_i(t) \ll N$  for all nodes. This means that each node has already had a large number of contacts, but that number is not too large, so that the integrated network cannot be considered as a complete graph, i.e., it is still sparse. In the limit of large  $N$  there is clearly a large temporal interval such that this condition is fulfilled. The condition  $1 \ll k_i(t) \ll N$  allows us to replace in Eq. (8)  $N - k_i(t) - 1$  with  $N$  and  $p(k_i)$  with  $(k_i(t))^{-\beta}$ . Considering only leading terms Eq. (8) becomes

$$\partial_t \rho_i(t) = -\mu \rho_i(t) + \lambda [1 - \rho_i(t)] \sum_j A_{ij}(t) \left( \frac{a_i}{k_i} + \frac{a_j}{k_j} \right) \rho_j(t). \quad (9)$$

### The linking probability

To proceed further we perform the equivalent of the heterogeneous mean-field approximation for static networks, i.e., we replace the time-integrated adjacency matrix  $A_{ij}(t)$  with its annealed form,  $P_{ij}(t)$ , i.e., the proba-

bility that  $v_i$  and  $v_j$  have been in contact in the past. The evolution of  $P_{ij}(t)$  is described by the master equation:

$$\partial_t P_{ij}(t) = \left[ \frac{a_i p(k_i)}{N - k_i - 1} + \frac{a_j p_j(k_j)}{N - k_j - 1} \right] [1 - P_{ij}(t)]. \quad (10)$$

In Eq. (10)  $P_{ij}$  grows either because the node  $v_i$  activates (probability per unit time  $a_i$ ), it creates a new connection [probability  $p(k_i)$ ] and the new partner is  $v_i$  [probability  $(N - k_i - 1)^{-1}$ ] or because of the event with the role of  $v_i$  and  $v_j$  interchanged.

In the temporal interval of interest we can use again the relations holding for large times  $p(k_i) \approx k_i^{-\beta}$  and  $N - k_j - 1 \approx N$ . Moreover, for large times, the degree of a node of activity  $a_i$  can be estimated by its average value  $\bar{k}(a_i, t)$ , given by Eq. (2). So we obtain

$$\partial_t P_{ij}(t) = [1 - P_{ij}(t)] \frac{g(a_i) + g(a_j)}{N t^{\frac{\beta}{1+\beta}}}, \quad (11)$$

---


$$\partial_t \rho(a, t) = -\mu \rho(a, t) + \lambda [1 - \rho(a, t)] \left\{ \frac{ag(a)}{g(a)+\langle g \rangle} \int da' F(a') \rho(a', t) + \frac{a}{g(a)+\langle g \rangle} \int da' F(a') \rho(a', t) g(a') + g(a) \int da' F(a') \frac{a'}{g(a')+\langle g \rangle} \rho(a', t) + \int da' F(a') \frac{a' g(a')}{g(a')+\langle g \rangle} \rho(a', t) \right\} \quad (15)$$

where we have replaced the sums over nodes with integrals over the activities  $1/N \sum_j \rightarrow \int da' F(a')$  and used Eq. (3), which can be rewritten as

$$C(a) = (1 + \beta) [g(a) + \langle g \rangle]. \quad (16)$$

Eq. (15) is effectively an ABMF approach, since all the information on the behavior of the node  $v_i$  depends on its activity  $a_i$ . Note that, although Eqs. (8) and (9) described the dynamics of the individual node, the further approximation underlying Eq. (10) has transformed the approach into an ABMF one, conceptually analogous to the heterogeneous mean-field approximation on static networks, where all the information on node  $v_i$  is encoded in its degree  $k_i$ .

It is important to remark that in Eq. (9) the time dependencies of  $P(a_i, a_j, t) \propto t^{1/(1+\beta)}$  and of the average degree  $\bar{k}(a_i, t) \propto t^{1/(1+\beta)}$  cancel out, so that the right hand side of Eq. (15) does not depend explicitly on time. This suggests that in this temporal regime the epidemic can be seen as an activity-driven process taking place on an effective static graph, where the probability for nodes  $v_i$  and  $v_j$  to be linked is given by Eq. (14) and the quantity  $t^{1/(1+\beta)}/N$  is a fixed quantity  $\tau$  whose value only

where we have defined

$$g(a_i) = a_i / [C(a_i)]^\beta. \quad (12)$$

Eq. (11) can be readily solved, yielding

$$P_{ij}(t) = 1 - e^{-\frac{(1+\beta)t^{1/(1+\beta)}}{N} [g(a_i) + g(a_j)]} \quad (13)$$

In the regime  $t^{1/(1+\beta)} \ll N$ ,  $P_{ij}(t)$  becomes

$$P_{ij}(t) = (1 + \beta) \frac{t^{1/(1+\beta)}}{N} [g(a_i) + g(a_j)]. \quad (14)$$

Notice that  $P_{ij}(t)$  is a topological feature of the activity-driven network, independent of the epidemic process.

#### Asymptotic ABMF equation

We now introduce into Eq. (9) the annealed expression for the integrated adjacency matrix  $A_{ij}(t) \approx P_{ij}(t) = P(a_i, a_j, t)$  and for the connectivity  $k_i(t) = \bar{k}(a_i, t)$ . In this way the equations depend on the nodes  $v_i$  and  $v_j$  only through their activities  $a_i$  and  $a_j$ . The equation for the probability  $\rho(a, t)$  that a generic node of activity  $a$  is infected at time  $t$  is therefore:

determines the average degree of the network. Performing simulations over an ensemble of these effective static networks and averaging the results one should then reproduce the predictions of the ABMF approach, Eq. (15).

From Equation (15), by performing a linear stability analysis around the absorbing state  $\rho(a, t) = 0$  (see Appendix), it is possible to compute analytically the epidemic threshold  $(\lambda/\mu)_c$ , for any value of the reinforcement parameter  $\beta$  and of the exponent of the analytical distribution  $\nu$ . Since for large times the node degrees diverge and correlations can be neglected, we expect the linear stability analysis to provide the correct estimate of the epidemic threshold when the epidemics start at very long times i.e. when the degrees  $k_i(t)$  have already become very large.

The results of the linear stability analysis are presented in Fig. 1 showing that the thresholds are smaller than in the memoryless case. This lower value is a consequence of the fact that memory reinforces the activity fluctuations, and in these models fluctuations clearly reduce the epidemic threshold, as shown by Eq. (7). The effect can be simply understood since nodes with large activity have also a large degree, therefore they are easily involved in epidemic contacts not only because they are frequently

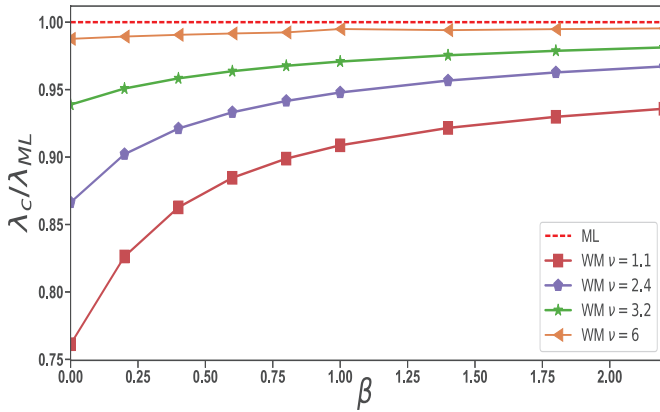


Figure 1. Plot of the ratio  $\lambda_c/\lambda_{ML}$  between the epidemic thresholds in the memory (WM) and in the memoryless (ML) cases, for different values of the exponent  $\nu$  of the distribution  $F(a) = Ba^{-(\nu+1)}$ . The dashed line is the mean-field memoryless results, while the solid lines are the outcomes of the ABMF equations in presence of memory.

activated but also because they are frequently contacted by other nodes. In this way memory reinforces the effect of activity fluctuations. In this framework, Fig. 1 also shows that at large  $\nu$  i.e. for increasingly smaller fluctuations, the difference with the memoryless model vanishes. In particular, for  $F(a) = \delta(a - a_0)$  i.e. when the activity does not fluctuate, one obtains from Eq.(15)  $\partial_t \rho(t) = -\mu \rho(t) + 2a_0 \lambda [1 - \rho(t)]$  that is the same equation of the memoryless case. This also explains the quite surprising observation that the threshold is a growing function of  $\beta$ , converging to the memoryless case as  $\beta \rightarrow \infty$ . Indeed, the tail of the degree distribution decays at large  $k$  as  $k^{-[(1+\beta)\nu+1]}$  [21], therefore at large  $\beta$  we get a faster decay and smaller degree fluctuations. For the same reason, in the limit  $\beta \rightarrow 0$  the difference with the memoryless case is maximal, since degree inhomogeneities are stronger in this case.

We remark that in Eq. (15), as in the memoryless case, dynamical correlations are ignored. However, we expect that at finite times, due to the finite connectivity of the integrated graph, the effect of correlations becomes important. The memory process leads to the formation of small clusters of mutually connected high activity vertices, which become reservoirs of the disease in the SIS model. The high frequency of mutual contacts allows for reinfection, favouring the overall survival of the epidemic spreading in the system. In this way, social circles with high activity play a role analogous to that played by the max K-core or the hub and its immediate neighbors for SIS epidemics in static networks [38, 39]. To clarify the effect of dynamical correlations at finite time, in the next Section we compare the analytical predictions with results of numerical simulations. As a final remark, we note that, in the asymptotic ABMF approach, the linear stability analysis also holds for the SIR model, imply-

ing that the epidemic threshold is the same of the SIS model. However, in the SIR model reinfection is not allowed so that the initial presence of small clusters of mutually connected high activity vertices effectively inhibits the spread of the disease. For this reason, we expect that finite connectivity (i.e. finite time) increases the epidemic threshold with respect to the mean-field result, as we will check in numerical simulations.

## IV. NUMERICAL SIMULATIONS

### SIS model on the effective static network

As discussed above, Eq. (15) can be interpreted as a heterogeneous mean-field equation for a SIS epidemic on an effective static network where the probability that  $v_i$  and  $v_j$  are connected is

$$P_{ij} = P(a_i, a_j) = \tau(1 + \beta)[g(a_i) + g(a_j)]. \quad (17)$$

Here  $\tau \ll 1$  is a constant,  $g(a) = a/[C(a)]^\beta$  and  $C(a)$  is a function that can be evaluated numerically for  $\beta > 0$ , while for  $\beta = 0$  it takes the simple form  $C(a) = a + \langle a \rangle$ . The constant  $\tau$  can be tuned in order to set the average degree of the network, because

$$k(a) = N \int da' F(a') P(a, a') = (1 + \beta) N \tau [g(a) + \langle g \rangle], \quad (18)$$

so that

$$\langle k \rangle = \int da' F(a') k(a') = 2(1 + \beta) N \tau \langle g \rangle. \quad (19)$$

We now study the SIS epidemic evolution on the effective static network.

Given the activity of each node, extracted according to the distribution  $F(a)$ , for each of the possible pairs of nodes we place an edge with probability given by Eq. (17). On top of this quenched topology we run a memoryless activity-driven SIS dynamics, starting with 10% of the nodes in the infected state, until the stationary state is reached and we record the fraction of infected nodes. We repeat the procedure many times for each value of  $\lambda$ , while  $\mu$  is fixed to 0.015. We determine the threshold as the position of the maximum of the susceptibility [40]  $\chi = N(\overline{\rho^2} - \overline{\rho}^2)/\overline{\rho}$ , where the overbar denotes the average over dynamical realizations at fixed topology. We repeat all this for several networks obtained using different sequences of activities and different samplings of  $P_{ij}$  and we average the epidemic thresholds found for each of them.

We first check that, as long as  $1 \ll \langle k \rangle \ll N$ , the results are independent of the exact value of  $\langle k \rangle$ , as predicted by the theory. Fig. 2 shows, for  $\beta = 1$ , that the effective threshold initially grows with  $\langle k \rangle$  but then reaches a plateau, in accordance with the expectations.

In Fig. 3 we report the dependence of the effective epidemic threshold as a function of  $\beta$  for three values of the

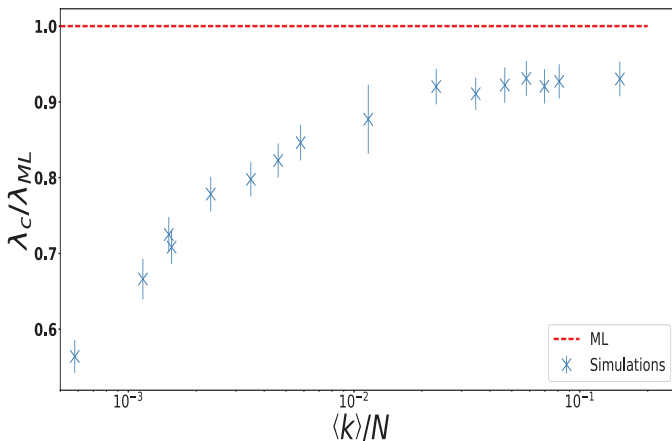


Figure 2. SIS model on the effective static network:  $\nu = 2.4$ ,  $\epsilon = 0.01$ ,  $\mu = 1.5 \cdot 10^{-2}$  and  $N = 10^4$ . Ratio between the epidemic threshold found in simulations and the result of the memoryless model in Eq.(7), as a function of  $\log(\langle k \rangle / N)$ . For  $\langle k \rangle / N > 0.01$ , we observe practically no dependence on  $\langle k \rangle$ .

average degree  $\langle k \rangle$ , compared with the predictions of the ABMF theory with and without memory. We observe that, as  $\langle k \rangle$  grows, numerical results tend to coincide with theoretical predictions. A nice agreement with the ABMF results is obtained for  $\langle k \rangle \approx 100$ , which is a large but realistic number of connections in a social systems. We remark that  $\langle k \rangle \approx 100$  is large enough for observing mean field behavior but also it is much smaller than the total number of sites  $N = 5 \cdot 10^4$  so that the system is not fully connected and degree fluctuations are important. On the other hand, for small values of  $\langle k \rangle$  the value of the threshold is smaller than the one predicted theoretically. Indeed, on effective static networks with small connectivity we expect the presence of clusters of mutually interconnected nodes to be relevant, as they are able to reinfect each other several times. It is well known that for the SIS model these backtracking effects tend to lower the epidemic threshold since social circles with high activity favor the overall survival of the epidemic.

### Epidemics on time-evolving networks

Let us now consider simulations of the epidemic spreading on the full time evolving network. We consider a graph of size  $N = 5 \cdot 10^4$  with activity distributed according to  $F(a) = Ba^{-(\nu+1)}$  ( $\nu = 2.4$ ) and a cutoff  $\epsilon = 10^{-2}$ . To extract the activities of individual nodes we perform an importance sampling so that, even in the finite size system, the moments  $\langle a \rangle$  and  $\langle a^2 \rangle$  coincide with their expected values.

We first start the temporal evolution of the network and at a later time  $t_0$  we let the epidemic begin. We evaluate at  $t_0$  the average connectivity of the nodes  $\langle k \rangle_0$  which measures the evolution of the network at the starting time. In both the SIS and SIR models, we use two

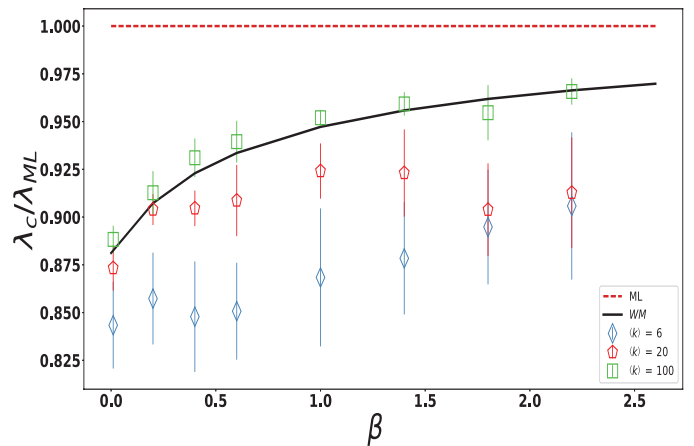


Figure 3. SIS model on the effective static network. Ratio between the epidemic threshold with memory and the epidemic threshold of the memoryless case as a function of the reinforcement parameter  $\beta = [0.01, 0.2, 0.4, 0.6, 1, 1.4, 1.8, 2.2]$ , with  $\nu = 2.4$ ,  $\epsilon = 0.01$ ,  $\mu = 1.5 \cdot 10^{-2}$ ,  $N = 5 \cdot 10^4$ . The points are averages of different realizations of the network with different sequences of activity  $a_1, a_2, \dots, a_N$ : 32 realizations for  $\langle k \rangle = 6$ , 16 realizations for  $\langle k \rangle = 20$ , 4 realizations for  $\langle k \rangle = 100$

different initial conditions. The first is to randomly select (RA) the node to infect at time  $t_0$ , while the second is to infect the most active node (MA) at time  $t_0$ . We keep the recovery rate fixed at  $\mu = 1.5 \cdot 10^{-2}$  and vary the probability of infection  $\lambda$  to study the dependence of its critical value on the memory parameter  $\beta$ .

### SIS model

In the SIS model, we determine the epidemic threshold using the lifespan method [41]. We plot (see Fig. 4), as a function of the parameter  $\lambda$ , the average lifespan of simulations ending before the coverage (i.e., the the fraction of distinct sites ever infected) reaches a preset value that we take equal to  $1/2$ . The threshold is estimated as the value of  $\lambda$  for which the lifespan has a peak.

The epidemic thresholds of numerical simulations are compared with theoretical predictions in Fig. 5 (RA case) and 6 (MA case). Numerical results converge toward the analytical prediction as  $\langle k \rangle_0$  becomes larger, while there are strong deviations for small  $\langle k \rangle_0$ .

For small  $\langle k \rangle_0$  two competing effects are at work. First, infections are mediated by an effective static network with small connectivity, therefore we expect backtracking effects to enhance epidemic spreading and to lower the threshold. Second, for small  $\langle k \rangle_0$ , moves connecting new partners are also possible. In these moves nodes are chosen randomly in the whole system according to a memoryless dynamics, which displays a higher epidemic threshold. So there exists a competition between backtracking correlations and memoryless moves which re-

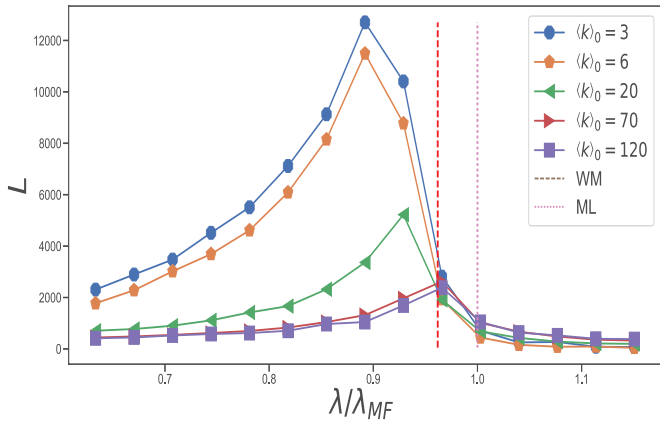


Figure 4. SIS epidemic process on the activity driven network MA. Lifespan ( $L$ ) as function of the ratio between the epidemic threshold with memory and the epidemic threshold of the memoryless for different values of  $\langle k \rangle_0$ .  $N = 5 \cdot 10^4$ ,  $\nu = 2.4$ ,  $a \in [10^{-2}, 1]$ . We consider  $4 \cdot 10^3$  epidemic realizations for each value of  $\lambda$ . Dynamics starts from the most active site and at small  $\langle k \rangle_0$  back-tracking effects are dominant favouring the epidemic spreading; this on one side lowers the value of the threshold (value of  $\lambda$  corresponding to the peak) but also increases the lifespan of the system at small  $\lambda$ .

duce and increase the threshold, respectively. Clearly for large  $\langle k \rangle_0$  both effects become negligible and the ABMF result is recovered.

Figs. 5 and 6 show that at large  $\beta$  backtracking effects (leading to small thresholds) are strong when the evolution starts from the most active site, while they are negligible with random initial conditions. The most active node indeed has the largest degree and she forms a cluster of highly activated nodes where the high frequency of mutual contacts allows for reinfections and positive correlations. Conversely, the average site has a small connectivity and can activate new links with high probability giving rise essentially to a memoryless epidemic dynamics.

The case  $\beta = 0$  coincides with the memoryless case (ML) and the dynamics never occurs on the effective static network. Figures 5-6 show that at very small  $\beta$ , even for the largest considered value  $\langle k \rangle_0 = 120$ , the creation of new links dominates the dynamics increasing the epidemic threshold towards the memoryless case. However, we expect that for large enough  $\langle k \rangle_0$ , at any  $\beta > 0$ , the dynamics is dominated by memory and infections spread on the effective static network recovering the ABMF result. This originates a singular behavior where the limits  $\beta \rightarrow 0$  and  $\langle k \rangle_0 \rightarrow \infty$  do not commute.

#### SIR model

The results of simulations of the SIR process are displayed in Fig. 7 and Fig 8 for the RA and MA case

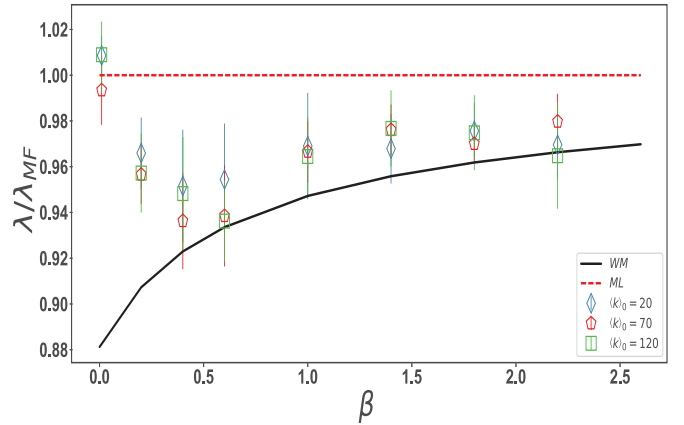


Figure 5. SIS epidemic process on the activity driven network, RA. Ratio between the epidemic threshold with memory and the epidemic threshold of the memoryless case as a function of the reinforcement parameter  $\beta = [0.01, 0.2, 0.4, 0.6, 1, 1.4, 1.8, 2.2]$ .  $N = 5 \cdot 10^4$ ,  $\nu = 2.4$ ,  $a \in [10^{-2}, 1]$ . The dotted line represents the memoryless result (ML), the solid line is the analytical prediction obtained from Eq. (15) in the memory case (WM). We consider  $4 \cdot 10^3$  epidemic realizations for each value of  $\lambda$ .

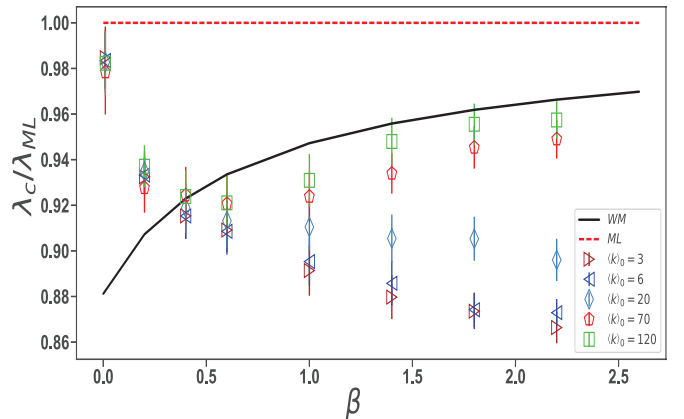


Figure 6. SIS epidemic process on the activity driven network, MA. Ratio between the epidemic threshold with memory and the epidemic threshold of the memoryless case as a function of the reinforcement parameter  $\beta = [0.01, 0.2, 0.4, 0.6, 1, 1.4, 1.8, 2.2]$ .  $N = 5 \cdot 10^4$ ,  $\nu = 2.4$ ,  $a \in [10^{-2}, 1]$ . The dotted line represents the memoryless result (ML), the solid line is the analytical prediction obtained from Eq. (15) (WM). We consider  $4 \cdot 10^3$  epidemic realizations for each value of  $\lambda$ .

respectively. The threshold is estimated from the peak of the variability  $\Delta = \sqrt{\langle N_R^2 \rangle - \langle N_R \rangle^2} / \langle N_R \rangle$ , i.e., the standard deviation of the number of recovered nodes  $N_R$  at the end of the simulation [42]. As for SIS, at large  $\langle k \rangle_0$  dynamical correlations can be neglected and simulations recover the ABMF result. Simulations clearly show



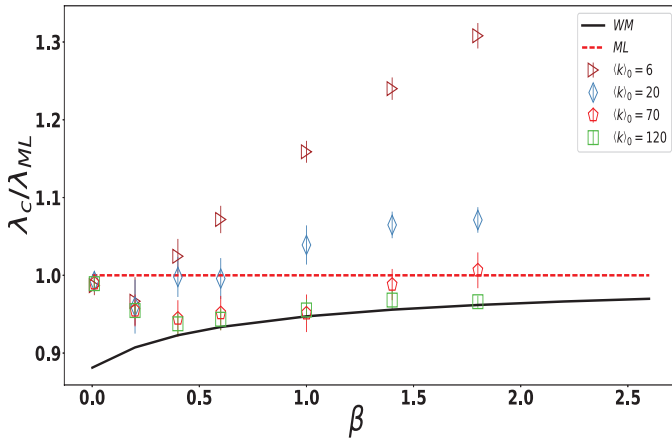


Figure 7. SIR epidemic process on the activity driven network, RA. Ratio between the epidemic threshold with memory and the epidemic threshold of the memoryless case as a function of the reinforcement parameter  $\beta = [0.01, 0.2, 0.4, 0.6, 1, 1.4, 1.8]$ .  $N = 5 \cdot 10^4$ ,  $\nu = 2.4$ ,  $a \in [10^{-2}, 1]$ . The dotted line represents the memoryless result (ML), the solid line is the analytical prediction obtained from Eq. (15) in the memory case (WM). We consider  $2 \cdot 10^3$  epidemic realizations for each value of  $\lambda$ .

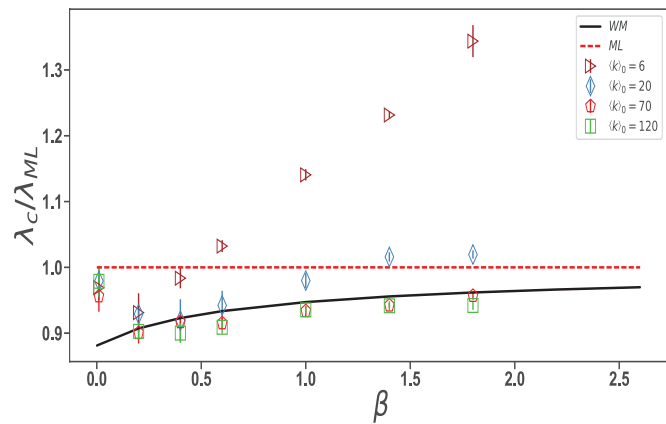


Figure 8. SIR epidemic process on the activity driven network, MA. Ratio between the epidemic threshold with memory and the epidemic threshold of the memoryless case as a function of the reinforcement parameter  $\beta = [0.01, 0.2, 0.4, 0.6, 1, 1.4, 1.8]$ .  $N = 5 \cdot 10^4$ ,  $\nu = 2.4$ ,  $a \in [10^{-2}, 1]$ . The dotted line represents the memoryless result (ML), the solid line is the analytical prediction obtained from Eq. (15) in the memory case (WM). We consider  $4 \cdot 10^3$  epidemic realizations for each value of  $\lambda$ .

that now correlations at small  $\langle k \rangle_0$  inhibit the epidemic spreading and the critical threshold becomes larger. As in the SIS model, at small  $\beta$  the memory is negligible and the dynamics is driven by the creation of new links, so that the threshold values are close to the memoryless case (ML), even if for any  $\beta > 0$  we expect for large enough  $\langle k \rangle_0$  a convergence to the ABMF prediction. On

the other hand, for larger  $\beta$ , the epidemics evolves on the integrated network, dynamical correlations become important and the thresholds grow even larger than in the memoryless case.

## V. CONCLUSIONS

The analytical and numerical results presented in this paper provide a complete understanding of the interplay between the temporal evolution of the activity-driven network with memory and the epidemic process occurring on top of it. The time when the epidemic process begins has crucial consequences. In the long time limit the reinforcement mechanism of the topological evolution completely inhibits the formation of new connections. If the activity-driven epidemic dynamics starts at this stage, it takes place on a topology which is in practice static. All nodes have a very large number of connections and this makes mean-field theory asymptotically exact. The epidemic threshold, which is the same for SIS and SIR dynamics, is reduced with respect to the memoryless case, because memory enhances the effect of activity fluctuations.

If instead the epidemic process starts before memory has completely taken over, interesting model-dependent preasymptotic effects are observed. The fundamental observation is that at this stage nodes with large activity tend to interact with their social circles, while less active nodes still tend to explore the system creating new connections. The first type of interaction tends to enhance SIS spreading, while the second tends to suppress it. This leads to positive or negative corrections to the asymptotic value of the threshold, depending on the initial conditions and on the reinforcement parameter  $\beta$ . In the SIR case instead, since reinfection is not possible, the interaction within social circles is strongly detrimental for the epidemic propagation, so that the asymptotic value of the threshold is always reached from above. Our results allow to fully understand the contrasting effects of strong ties on SIS and SIR dynamics observed in Ref. [31], and it opens new possibilities in control of epidemic spreading on temporal networks with high correlations.

Several possible extensions of the model considered here are possible to make it more realistic, both in terms of the topological evolution and of the spreading process. Among them probably the most interesting would be the inclusion of burstiness in agents activity. The combined effect on activity-driven models of tie reinforcement and non exponentially-distributed interevent times has been studied in Refs. [22, 43]. The inclusion of a spreading dynamics in this framework is a promising and challenging avenue for future research.

\*

## Appendix A: Linear Stability Analysis

The dynamical process is described by the ABMF equation [Eq. (15)] which we rewrite as

$$\partial_t \rho(a) = -\mu \rho(a) + \lambda [1 - \rho(a)] [A(a)g(a) \langle \rho(a) \rangle + A(a) \langle g(a)\rho(a) \rangle + g(a) \langle A(a)\rho(a) \rangle + \langle A(a)g(a)\rho(a) \rangle], \quad (\text{A1})$$

where for simplicity we have omitted the time dependencies and defined  $A(a) = a/[g(a) + \langle g(a) \rangle]$ .

To study the stability of the system linearized around the fixed point  $\rho(a) = 0$ , we introduce the following functions

$$\begin{aligned} \rho &= \langle \rho(a) \rangle \\ x &= \langle g(a)\rho(a) \rangle \\ y &= \langle A(a)\rho(a) \rangle \\ z &= \langle A(a)g(a)\rho(a) \rangle \end{aligned} \quad (\text{A2})$$

Integrating Eq. (A1) over  $a$  and keeping only linear terms in  $\rho(a)$  we obtain an equation for  $\partial_t \rho$ . Similarly, multiplying Eq. (A1) by  $g(a)$  and integrating over  $a$  we get an equation for  $\partial_t x$ . Doing the same for  $y$  and  $z$  we obtain a closed system of four equations for four variables

$$\begin{aligned} \partial_t \rho &= -\mu \rho + \lambda [\langle A(a)g(a) \rangle \rho + \langle A(a) \rangle x + \langle g(a) \rangle y + z] \\ \partial_t x &= -\mu x + \lambda [\langle A(a)g^2(a) \rangle \rho + \langle A(a)g(a) \rangle x + \langle g^2(a) \rangle y + \langle g(a) \rangle z] \\ \partial_t y &= -\mu y + \lambda [\langle A^2(a)g(a) \rangle \rho + \langle A^2(a) \rangle x + \langle A(a)g(a) \rangle y + \langle A(a) \rangle z] \\ \partial_t z &= -\mu z + \lambda [\langle A^2(a)g^2(a) \rangle \rho + \langle A^2(a)g(a) \rangle x + \langle A(a)g^2(a) \rangle y + \langle A(a)g(a) \rangle z] \end{aligned} \quad (\text{A3})$$

These equations describe the epidemic near the state  $\rho(a) = 0$  and the jacobian matrix of this system of equations is

$$J = \begin{pmatrix} \lambda \langle Ag \rangle - \mu & \lambda \langle A \rangle & \lambda \langle g \rangle & \lambda \\ \lambda \langle Ag^2 \rangle & \lambda \langle Ag \rangle - \mu & \lambda \langle g^2 \rangle & \lambda \langle g \rangle \\ \lambda \langle A^2 g \rangle & \lambda \langle A^2 \rangle & \lambda \langle Ag \rangle - \mu & \lambda \langle A \rangle \\ \lambda \langle A^2 g^2 \rangle & \lambda \langle A^2 g \rangle & \lambda \langle Ag^2 \rangle & \lambda \langle Ag \rangle - \mu \end{pmatrix} \quad (\text{A4})$$

The state  $\rho(a) = 0$  is stable provided all eigenvalues of  $J$  are negative, hence the epidemic threshold is given by the value  $(\lambda/\mu)_c$  such that largest eigenvalue of the jacobian matrix is zero. Numerical evaluation of the matrix  $J$  and of its eigenvalues can be obtained, first by solving numerically Eq. (3) to get  $C(a)$  and  $g(a)$  and then calculating the averages defining  $J$ .

- 
- [1] P. Holme and J. Saramäki, Phys. Rep. **519**, 97 (2012).
  - [2] D. Balcan, V. Colizza, B. Goncalves, H. Hu, J. J. Ramasco, and A. Vespignani, PNAS **106**, 21484 (2009).
  - [3] A. Barrat, M. Barthélemy, and A. Vespignani, *Dynamical processes on complex networks* (Cambridge University Press, 2008).
  - [4] S. Eubank, H. Guclu, V. S. Kumar, M. V. Marathe, A. Srinivasan, Z. Toroczkai, and N. Wang, Nature **429**, 180 (2004).
  - [5] E. Agliari, R. Burioni, D. Cassi, and F. M. Neri, Phys. Rev. E **73**, 046138 (2006).
  - [6] P. Bajardi, A. Barrat, F. Natale, L. Savini, and V. Colizza, PLoS ONE **6**, e19869 (2011).
  - [7] E. Valdano, M. R. Fiorentin, C. Poletto, and V. Colizza, Phys. Rev. Lett. **120**, 068302 (2018).
  - [8] C. Cattuto, W. Van den Broeck, A. Barrat, V. Colizza, J.-F. Pinton, and A. Vespignani, PLoS ONE **5**, e11596 (2010).
  - [9] J. Saramäki and E. Moro, Eur. Phys. Jour. B **88**, 164 (2015).
  - [10] N. Perra, B. Gonçalves, R. Pastor-Satorras, and A. Vespignani, Sci. Rep. **2**, 469 (2012).
  - [11] N. Perra, A. Baronchelli, D. Mocanu, B. Goncalves, R. Pastor-Satorras, and A. Vespignani, Phys. Rev. Lett. **109**, 238701 (2012).
  - [12] M. Starnini and R. Pastor-Satorras, Phys. Rev. E **89**, 032807 (2014).
  - [13] A. Rizzo and M. Porfiri, Eur. Phys. J. B **89**, 20 (2016).
  - [14] M. S. Granovetter, Am. J. Sociol. **78**, 1360 (1973).
  - [15] G. Miritello, R. Lara, M. Cebrian, and E. Moro, Sci. Rep. **3**, 1950 (2013).
  - [16] J. Saramäki, E. A. Leicht, E. López, S. G. B. Roberts, F. Reed-Tsochas, and R. I. M. Dunbar, PNAS **111**, 942 (2014).
  - [17] R. I. M. Dunbar, J. Hum. Evol. **22**, 469 (1992).
  - [18] J. Stiller and R. I. M. Dunbar, Soc. Netw. **29**, 93 (2007).
  - [19] M. Karsai, N. Perra, and A. Vespignani, Sci. Rep. **4**, 4001 (2014).
  - [20] H. Kim, M. Ha, and H. Jeong, Eur. Phys. J. B **88**, 315 (2015).
  - [21] E. Ubaldi, N. Perra, M. Karsai, A. Vezzani, R. Burioni, and A. Vespignani, Sci. Rep. **6**, 35724 (2016).
  - [22] R. Burioni, E. Ubaldi, and A. Vezzani, J. Stat. Mech. Theory Exp. **2017**, 054001 (2017).

- [23] H. Kim, M. Ha, and H. Jeong, *Phys. Rev. E* **97**, 062148 (2018).
- [24] M. Rosvall, A. V. Esquivel, A. Lancichinetti, J. D. West, and R. Lambiotte, *Nat. Commun.* **5**, 4630 (2014).
- [25] I. Scholtes, N. Wider, R. Pfitzner, A. Garas, C. J. Tesse, and F. Schweitzer, *Nat. Commun.* **5**, 5024 (2014).
- [26] S. Liu, N. Perra, M. Karsai, and A. Vespignani, *Phys. Rev. Lett.* **112**, 118702 (2014).
- [27] R. Lambiotte, V. Salnikov, and M. Rosvall, *J. Complex Networks* **3**, 177 (2015).
- [28] M. Karsai, M. Kivelä, R. K. Pan, K. Kaski, J. Kertész, A.-L. Barabási, and J. Saramäki, *Phys. Rev. E* **83**, 025102 (2011).
- [29] M. Karsai, K. Kaski, and J. Kertész, *PLoS One* **7**, e40612 (2012).
- [30] I. Pozzana, K. Sun, and N. Perra, *Phys. Rev. E* **96**, 042310 (2017).
- [31] K. Sun, A. Baronchelli, and N. Perra, *Eur. Phys. J. B* **88**, 326 (2015).
- [32] A. Moinet, M. Starnini, and R. Pastor-Satorras, *Phys. Rev. Lett.* **114**, 108701 (2015).
- [33] M. Henkel and M. Pleimling, *Non-Equilibrium Phase Transitions Volume 2: Ageing and Dynamical Scaling Far from Equilibrium* (Springer Netherlands, 2010).
- [34] M. Starnini and R. Pastor-Satorras, *Phys. Rev. E* **87**, 062807 (2013).
- [35] R. Pastor-Satorras and A. Vespignani, *Phys. Rev. Lett.* **86**, 3200 (2001).
- [36] S. N. Dorogovtsev, A. V. Goltsev, and J. F. F. Mendes, *Rev. Mod. Phys.* **80**, 1275 (2008).
- [37] R. Pastor-Satorras, C. Castellano, P. Van Mieghem, and A. Vespignani, *Rev. Mod. Phys.* **87**, 925 (2015).
- [38] C. Castellano and R. Pastor-Satorras, *Sci. Rep.* **2**, 371 (2012).
- [39] C. Castellano and R. Pastor-Satorras, *Phys. Rev. X* **7**, 041024 (2017).
- [40] S. C. Ferreira, C. Castellano, and R. Pastor-Satorras, *Phys. Rev. E* **86**, 041125 (2012).
- [41] M. Boguñá, C. Castellano, and R. Pastor-Satorras, *Phys. Rev. Lett.* **111**, 068701 (2013).
- [42] P. Shu, W. Wang, M. Tang, and Y. Do, *Chaos* **25**, 063104 (2015).
- [43] E. Ubaldi, A. Vezzani, M. Karsai, N. Perra, and R. Burioni, *Sci. Rep.* **7**, 46225 (2017).